1-21-2024

Modifying Peptide/Lipid-Associated Nucleic Acids (PLANAs) for CRISPR/Cas9 Ribonucleoprotein Delivery

Abdulelah Alhazza
Chapman University, alhazza@chapman.edu

Parvin Mahdipoor
Chapman University, mahdi102@mail.chapman.edu

Ryley Hall
Chapman University, hall222@mail.chapman.edu

Arthur Manda
Chapman University

Sandeep Lohan
Chapman University, lohan@chapman.edu

See next page for additional authors

Recommended Citation

Alhazza, A., Mahdipoor, P., Hall, R., et al., 2024. Modifying peptide/lipid-associated nucleic acids (PLANAs) for CRISPR/Cas9 ribonucleoprotein delivery. Eur. J. Pharm. Biopharm. 195, 106708. https://doi.org/10.1016/j.ejps.2024.106708

Modifying Peptide/Lipid-Associated Nucleic Acids (PLANAs) for CRISPR/Cas9 Ribonucleoprotein Delivery

Authors

Abdulelah Alhazza, Parvin Mahdipoor, Ryley Hall, Arthur Manda, Sandeep Lohan, Keykavous Parang, and Hamidreza Montazeri Aliabadi

European Journal of Pharmaceutical Sciences 195 (2024) 106708

Contents lists available at ScienceDirect

European Journal of Pharmaceutical Sciences

journal homepage: www.elsevier.com/locate/ejps

Modifying peptide/lipid-associated nucleic acids (PLANAs) for CRISPR/Cas9 ribonucleoprotein delivery

Abdulelah Alhazza [a,b,1], Parvin Mahdipoor [a,1], Ryley Hall [a], Arthur Manda [a], Sandeep Lohan [a], Keykavous Parang [a,c], Hamidreza Montazeri Aliabadi [a,c,*]

[a] Department of Biomedical and Pharmaceutical Sciences, Chapman University School of Pharmacy, Harry and Diane Rinker Health Science Campus, Irvine, CA 92618, USA

[b] Department of Pharmaceutics, Faculty of Pharmacy, Northern Border University, Rafha, 76313, Saudi Arabia

[c] Center for Targeted Drug Delivery, Chapman University School of Pharmacy, Harry and Diane Rinker Health Science Campus, Irvine, California 92618, USA

ARTICLE INFO

Keywords:
PLANA
CRISPR/Cas9
Polyethylene glycol
Lipids
In vitro
Transfection

ABSTRACT

With the first reports on the possibility of genome editing by Clustered Regularly Interspaced Short Palindromic Repeats (CRISPR) and CRISPR-associated protein (Cas)9 surfacing in 2005, the enthusiasm for protein silencing via nucleic acid delivery experienced a resurgence following a period of diminished enthusiasm due to challenges in delivering small interfering RNAs (siRNA), especially *in vivo*. However, delivering the components necessary for this approach into the nucleus is challenging, maybe even more than the cytoplasmic delivery of siRNA. We previously reported the birth of peptide/lipid-associated nucleic acids (PLANAs) for siRNA delivery. This project was designed to investigate the efficiency of these nanoparticles for *in vitro* delivery of CRISPR/Cas9 ribonucleoproteins. Our initial experiments indicated higher toxicity for PLANAs with the more efficient reverse transfection method. Therefore, polyethylene glycol (PEG) was added to the composition for PEGylation of the nanoparticles by partially replacing two of the lipid components with the PEG-conjugated counterparts. The results indicated a more significant reduction in the toxicity of the nanoparticle, less compromise in encapsulation efficiency and more PEGylation of the surface of the nanoparticles using DOPE-PEG2000 at 50 % replacement of the naïve lipid. The cell internalization and transfection efficiency showed a comparable efficiency for the PEGylated and non-PEGylated PLANAs and the commercially available Lipofectamine™ CRISPRMAX™. Next Generation Sequencing of the cloned cells showed a variety of indels in the transfected cell population. Overall, our results indicate the efficiency and safety of PEGylated PLANAs for *in vitro* transfection with CRISPR/Cas9 ribonucleoproteins. PEGylation has been studied extensively for *in vivo* delivery, and PEGylated PLANAs will be candidates for future *in vivo* studies.

1. Introduction

Nucleic acids are powerful tools in controlling gene and protein expression profiles. Despite the initial excitement and extensive efforts, however, the potential impact of these approaches is yet to be materialized fully in clinical settings. This is mainly due to the challenges in delivering RNA structures to the target cells, especially *in vivo*. Small interfering RNAs (siRNAs) and Clustered Regularly Interspaced Short Palindromic Repeats (CRISPR) and CRISPR-associated protein (Cas)9 have been the most extensively studied approaches for *in vivo* delivery of nucleic acids, which created a significant hype in the beginning of 20th century and early 2010s, respectively. The first clinical studies on CRISPR gene editing were performed in 2016 by injecting engineered T cells (transfected with CRISPR/Cas9 targeting PD-1) to a patient with metastatic non-small cell lung cancer (Cyranoski, 2016), and the 2020 Nobel Prize in Chemistry awarded to CRISPR/Cas9 research has added to the excitement for this approach.

Delivery of CRISPR/Cas9 reagents is either performed by delivering complexes of crispr RNA/ transactivating RNA and the Cas9 protein (called ribonucleoproteins or RNPs) (Mazurov et al., 2023), delivering Cas9 expressing mRNA and single guide RNA (sgRNA) (Ma et al., 2023), or by delivering a single vector consisting of Cas9 nuclease expression

* Corresponding author.
E-mail address: montazer@chapman.edu (H.M. Aliabadi).
[1] Equal contribution

https://doi.org/10.1016/j.ejps.2024.106708
Received 6 October 2023; Received in revised form 16 January 2024; Accepted 18 January 2024
Available online 21 January 2024

cassette and sgRNA cloning cassette (Liang et al., 2015). Either way, CRISPR/Cas9 delivery faces similar challenges as other nucleic acids, *in vitro* (rapid degradation, poor cellular internalization, etc.) and *in vivo*. The most successful nucleic acid delivery systems reported are lipid nanoparticles (LNPs) (Kazemian et al., 2022). However, even with this approach the efficiency of *in vivo* delivery needs to be improved (Behr et al., 2021). We first reported the birth of peptide/Lipid-Associated Nucleic Acids (PLANAs) in 2021 as a new approach in using lipid nanoparticles for siRNA delivery (Hall et al., 2021). In PLANAs, we replaced the positively charged component of LNPs (either a cationic or ionizable lipid) with a cyclic fatty acid conjugated peptide (CP-C18). The cyclic positively charged portion of the peptide comprised of 5 arginines to provide the positive charge required for interaction with negatively charged nucleic acids and two lysines for the sites of conjugation (R_5K_2). Two stearic acid (18 carbons) fatty acid chains were conjugated to the two lysines on the ring to facilitate interaction with the hydrophobic cell membrane and therefore, enhance cellular internalization. This specific peptide structure was selected after screening a library of linear (LP) and cyclic peptides (CP) conjugated to fatty acids with 2–18 carbon chains (C2–C18). These peptides were specifically designed for nucleic acid delivery, which demonstrated efficient *in vitro* siRNA delivery and silencing (Do et al., 2017). The structure of the selected peptide can be found in our previous publications (Hall et al., 2021; Do et al., 2017).

In the present study, we attempted CRISPR/Cas9 delivery via PLANAs. After a few unsuccessful attempts with the single vector system (results not included), we selected the RNP approach, which was more efficient. Our preliminary tests with the original PLANA formulation, however, showed significant toxicity when a reverse transfection approach was used. In this approach (despite the forward transfection usually used for siRNA in our lab) the nanoparticles are added to suspended cells at the time of seeding the cells (as opposed to adding them to attached cells after overnight incubation). To avoid this toxicity, we evaluated the effect of adding polyethylene glycol (PEG) to the nanoparticles. Many studies have reported that PEGylation of LNPs and other delivery systems could reduce cytotoxicity due to the hydrophilic nature of PEG that would cover the surface of nanoparticles (Casettari et al., 2010; Luong et al., 2016; Mattheolabakis et al., 2014; Shi et al., 2021; Zhang et al., 2014; Zheng et al., 2012). In the case of LNPs, PEGylation is usually performed by addition of a PEG-conjugated lipid to the nanoparticle composition (Suzuki and Ishihara, 2021). Therefore, we adapted the same strategy and investigated the effect of PEGylation of PLANAs via two different molecular weights for PEG (2000 and 5000) and by partially replacing DOPE or cholesterol with DOPE-PEG or cholesterol-PEG, respectively. The replacement was performed at different compositions, replacing 25, 50, or 75 % of the lipid molecules with the PEG-conjugated counterpart. We used human embryonic kidney HEK293 cells as the model cell line commonly used in proof-of-concept transfection studies, due to the ease of transfection. And finally, the model protein selected was hypoxanthine phosphoribosyl transferase (HPRT), a house-keeping protein commonly used as an endogenous protein with reliable and stable expression level in different tissues (Stewart et al., 2022; Zamani et al., 2020; Kweon et al., 2018; Gasperini et al., 2017).

2. Matrials and methods

Materials. The materials and instruments used in PLANA preparation have been reported elsewhere (Hall et al., 2021). Pegylated 1,2-Dioleoyl-sn-glycero-3-phosphoethanolamine (DOPE) was purchased from Nanosoft Polymers (Lewisville, NC) with two different molecular weights (DOPE-PEG2000-NH_2 and DOPE-PEG5000-NH_2). Pegylated cholesterol was supplied by Creative PEGWorks (Chapel Hill, NC), again with PEG molecular weights of 2 and 5 kD. The cell counting kit 8 (CCK8) reagent used in cytotoxicity evaluations was provided by Selleckchem Chemicals LLC (Houston, TX). Lipofectamine™ CRISPRMAX™ Cas9 Transfection Reagent (catalog no. CMAX00015), and Silencer Negative Control siRNA (catalog no. AM4635) were purchased from Life Technologies (Grand Island, NY, USA). The crispr RNA (Alt-R® CRISPR-Cas9 crRNA), transactivating RNA (Alt-R® CRISPR-Cas9 tracrRNA), Cas 9 nuclease (Alt-R™ S.p. Cas9 Nuclease V3), T7 endonuclease I (part of Alt-R® Genome Editing Detection Kit), and the primers used to amplify targeted region of the HPRT expressing gene were obtained from Integrated DNA Technologies (IDT, Coralville, IA). The sequence of the targeted region of the chromosome is presented in Supplementary Fig. 1. The KAPA HiFi HotStart ReadyMix (the DNA polymerase and nucleotides used in PCR reactions) was purchased from Roche Diagnostics (Indianapolis, IN). Malvern Nano ZS Zetasizer and disposable capillary cells were provided by Malvern Panalytical (Westborough, MA). Vectashield Vibrance with DAPI was supplied by Vector Laboratories (Burlingame, CA, USA). The DNA extraction kit, DNeasy Blood & Tissue Kit (Catalogue number: 69,504) was provided by Qiagen (Germantown, MD). All other consumables and reagents were obtained from VWR (Radnor, PA, USA).

Methods. The synthesis and characterization of peptides and PLANA preparation method are previously reported (Hall et al., 2021).

PLANA-PEG preparation. Non-PEGylated PLANAs were prepared according to the most effective composition reported previously (Hall et al., 2021). Briefly, cholesterol, phosphatidyl choline, and DOPE were added to ethanol and mixed, whereas nucleic acid and the CP-C18 peptide were mixed in the aqueous phase. The two phases were then mixed, and PLANA nanoparticles were formed by passing the mixture 50 times through a Mini Extruder (Avanti Lipids, Alabaster, Alabama) with a 100 nm filter to create nanoparticles around 100 nm. The ratio of ethanol to aqueous phase was 1:3. The ethanol was then removed by placing the nanoparticles via dialysis. The mole fraction of peptide, cholesterol, phosphatidyl choline, and DOPE were 0.0425, 0.1278, 0.2556, and 0.5741, respectively. We used two approaches to add polyethylene glycol (PEG) to the PLANA nanoparticles: replacing DOPE with DOPE-PEG and replacing cholesterol with cholesterol-PEG. We also evaluated the effect of two different PEG molecular weights (2000 and 5000 Daltons). PEGylated PLANAs were prepared with the exact same approach as the PLANAs. Briefly, the hydrophobic components (including PEGylated lipids) were mixed in ethanol, and peptide and Ribonucleoproteins (RNPs) or siRNA were dissolved in RNase-free water. The two phases were mixed, and the mixture was passed 50 times through 1 membrane with 100 nm pore size using a mini extruder (Avanti Polar Lipids; Alabaster, AL). The ethanol was removed using a dialysis bag with a molecular weight cut-off of 500–1000 Da (Biotech CE dialysis tubing). The level of PEGylation was controlled by the molar ratio of PEGylated lipid and non-PEGylate lipid incorporated into the formulation (*e.g.*, for 25, 50, and 75 % PEGylation, PEGylated: non-PEGylated molar ratios of 1:3, 1:1, and 3:1 were used, respectively).

Ribonucleoprotein (RNP) delivery. Commercially available Lipofectamine™ CRISPRMAX™ was used as a positive control, while saline and nanoparticles delivering negative control (scrambled) Crispr RNA were used as negative controls. The crRNA and tracrRNA were annealed in a nuclear-free Duplex Buffer (IDT, Coralville, IA) at 95 °C for 5 min and the duplexes were cooled down to ambient temperature. Cas9 enzyme was added to the duplex solution in 1:1 molar ratio (Cas9:RNA) and incubated at ambient temperature for 5 min to form the RNPs. RNPs were prepared fresh and kept on ice until incorporated into nanoparticles.

For delivery via Lipofectamine™ CRISPRMAX™, the manufacturer instructions were followed. Briefly, CAS9 PLUS™ reagent was mixed with RNPs in Opti-MEM medium in one Eppendorf microtube and Lipofectamine™ CRISPRMAXTM reagent was diluted in Opti-MEM medium in another tube. After 20 min of incubation at ambient temperature, the contents of the two tubes were mixed to form the complexes. As mentioned before, for PLANA and PLANA-PEG nanoparticles, the RNPs were added to the aqueous phase and nanoparticles were formed using the mini extruder.

Transfection was performed using both "forward" and "reverse" transfection methods. In "forward" transfection, cells were seeded, were incubated for 24 h to assure complete adherence, and then the nanoparticles were added to the wells. In "reverse" approach, however, the nanoparticles were placed in the wells first, and then the cell suspension was added to the wells, which afforded the nanoparticles an opportunity to interact with suspended cells, before the adherence was completed.

Encapsulation efficiency. To evaluate the effect of PEGylated lipids in the PLANA structure on the incorporation of nucleic acids, we studied the encapsulation efficiency of negative control (scrambled) siRNA using a dye exclusion assay using SYBR Green Dye II. We have previously reported using this method for the quantification of free siRNA (Hall et al., 2021; Do et al., 2017; Aliabadi et al., 2011). Briefly, freshly prepared PLANA dispersions (PEGylated or otherwise; RNA concentration = 100 nM) were placed in 96-well BD FluoroBlok MW Inserts, and a 1:10,000 diluted SYBR Green II dye solution was added to the samples. A SpectraMax M5 UV−Viz plate reader was used to quantify the fluorescence signal (λ excitation = 485 nm; λ emission = 527 nm). The siRNA concentrations were determined based on the strength of the signals using a standard curve created daily via pre-determined siRNA concentrations.

Surface charge determination. The ʒ-potential of the PLANAs can be an indication of the incorporation of PEGylated lipids in the PLANA structure. A Malvern Nano ZS Zetasizer and folded capillary cuvettes were used to measure the surface charge of the nanoparticles at 25 °C and 40 V using the Smoluchowski approximation. PLANA and PLAN-PEG dispersions (RNA-concentration = 100 nM) were used at different PEGylation levels.

Cell lines. Most of the experiments included in this study were performed in human embryonic kidney 293 (HEK293) cells (ATCC CRL-1573). The cytotoxicity of the siRNA-delivering nanoparticles was evaluated in MDA-MB-231 cells (ATCC HTB-26). Both cell lines were cultured, grown, and maintained in low glucose Dulbecco's modified Eagle's medium (DMEM) with 100 U/mL penicillin, 100 μg/mL streptomycin, and 10 % (v/v) FBS added. Cells were incubated at 37 °C and were exposed to 5 % CO_2 at all times. Cells were sub-cultured regularly when they were > 80 % confluent and were replaced with fresh population of thawed cells after 30 sub-cultures.

Cytotoxicity. The potential toxicity of the nanoparticles was evaluated by using CCK8 reagent as previously reported (Hall et al., 2021). Cytotoxicity experiments were performed using both "forward" and "reverse" transfection approaches. Briefly, HEK293 and MDA-MB-231 cells were seeded in 96-well plates (or were added to the wells containing the nanoparticles for the "reverse" approach) with a confluency of ~50 and 25 % (~400,000 and 150,000 cells/mL, or 40,000 and 15,000 cells per well), respectively. After 24 h incubation at 37 °C and exposure to 5 % CO_2 the nucleic acid-delivering nanoparticles were added to the wells in triplicate. For CRISPR/Cas9, four study groups were included representing nanoparticles delivering a final concentration of 2.5, 5, 10, and 20 nM of total RNA to each well. Only two study groups were evaluated for siRNA-delivering nanoparticles: 100 and 200 nM of siRNA. Cells were then incubated for 48 h in the same incubation conditions. After the incubation period, 10 μL of the CCK8 reagent was added to all the wells (including three wells for "Blank" wells that only contained cell-less medium) and the plates were incubated again for 60 min. SpectraMAX M5 UV−Viz Plate Reader was used to quantify the absorbance at 450 nm for each well. The signal quantified for "Blank" wells was subtracted from all measurements and the viability of the cells in each study group was calculated as a percentage compared to cells that only received normal saline (regarded as "No Treatment").

Cellular internalization. The internalization was assessed using reverse transfection and two methods to quantify and visually confirm the internalization using flow cytometry and confocal microscopy, respectively:

Flow Cytometry: CRISPR/Cas9 complexes were formed using ATTO-labeled tracrRNA and were delivered at a final concentration of 10 nM by Lipofectamine™ CRISPRMAX™, PLANAs, and PLANAs incorporating DOPE-PEG2000. After transferring the nanoparticles to 24-well plates (in triplicate), trypsinized HEK293 cells were added to each well (approximately 400,000 cells per mL or 160,000 cells per well) and were incubated under the same growth incubation conditions for 24 h. After this incubation period, the medium was removed from all wells, and cells were washed with sterile HBSS three times, before trypsinizing. Cells suspensions were pelleted at 600 rpm for 5 min and were resuspended in PBS. A FACSVERSE flow cytometer (BD Biosciences; San Jose, CA) was used to quantify the average fluorescence signal of the population of single intact cells. The percentage of fluorescent-positive cells was determined after calibrating the signal strength for ~ 1 % fluorescent-positive cells for the cells exposed to saline ("No Treatment").

Confocal Microscopy: In order to track and visualize the fluorescent signal inside the HEK293 cells, the internalization experiments were conducted with a similar approach in a 6-well plate. To grow cells on a coverslip that could be transferred to a slide, we placed sterilized coverslips at the bottom of all wells and to ensure cell adherence, added enough 10 % FBS to all wells to cover the entire surface of the coverslips. The plates were incubated at 37 °C for 30 min, after which the FBS was removed, nanoparticles were added, and cells were seeded in all wells. After 4 h of exposure to the nanoparticles and washing the cells with sterile HBSS (× 3), cells were fixed using 3.7 % formaldehyde in PBS. The cells were washed again (× 3), and the nuclei were stained with DAPI overnight. Confocal images were produced using Nikon A1R high-definition resonant scanning confocal microscope and NIS-Elements software (AR 4.30.02, 64bit).

Transfection. We selected HPRT, a housekeeping protein, as a model target. CrRNA was designed by IDT and primers to amplify the piece of DNA, including the targeted site via PCR was provided by the same company. The primers were designed in a way to amplify a 669 base-pair long amplicon, which is within the recommended 600–1000 base-pair range. It was also assured that the "cut site" targeted by crRNA was off-center, so the two resulting fragments after exposure to endonuclease were not similar in size. In the case of the primers used in this study, the resulting fragments were anticipated to be 471 and 198 base-pair long. DNA was extracted from HEK293 cells transfected with HPRT-targeting CRISPR/Cas9 using DNeasy Blood & Tissue Kit (Qiagen) and following the manufacturer's instructions. Briefly, cells were trypsinized, pelleted, and lysed in a lysis buffer. Proteinase K and Buffer AL were added, and the mixture was vortexed. After addition of ethanol and vortexing, the mixtures (including any precipitate) were transferred to spin columns and were centrifuged at 8000 rpm for 60 s. The flow-through and collecting tube were discarded. Then, Buffer AW1 was added to the spin column, and it was centrifuged again at 8000 rpm for 60 s to discard the flow-through. This step was repeated for Buffer AW2, and the column was centrifuged at 14,000 rpm for 3 min to discard the flow-through. The purified DNA was collected by adding Buffer AE and collecting the flow-through in a DNase-free tube after centrifuging at 8000 rpm for 60 s.

PCR was performed using KAPA HiFi HotStart DNA Polymerase (Roche), the forward and reverse primers, and PCR was performed for 30 cycles according to the guidelines provided by IDT. Alt-R Control A (a homoduplex; no T7 cleavage is expected) and Alt-R Control B (with a 6 base pair deletion compared to Control A) were added to each PCR run.

T7 endonuclease I (T7EI) was used to identify and cleave DNA mismatch caused by CRISPR/Cas9. PCR amplicons, Control A, and a 1:1 Control A:Control B mixture were exposed to T7EI (part of the Alt-R Genome Editing Detection Kit by IDT) following the manufacturer's instructions and were incubated at 37 °C for 60 min. The resulting samples were loaded in agarose gel, and gel electrophoresis was performed at 75 V and 400 mA for 75 min, along with a 75–20,000 ladder (GeneRuler I kb Plus DNA Ladder provided by ThermoFisher Scientific). Control A and mixture of Controls A and B (to create the mismatch) were

run as negative and positive controls for cleavage by T7EI, respectively, for all electrophoreses.

Cell cloning and DNA sequencing. To identify the gene edits, we required a pure transfected cell population (since the transfection was not achieved in 100 % of the cells). Cell cloning was performed using two approaches: a) Cloning cylinders: Naïve and transfected cell populations were sub-cultured in a petri dish with a very low population (10 - 25 cells/mL). After cells were adhered, the growth surface was monitored using a microscope, and single-cell areas were identified. PYREX® Cloning Cylinders (Corning, NY, USA) were used to isolate single cells. Cylinders were autoclaved before use and a sterile DOW Corning High Vacuum Grease (VWR) was used to secure the cylinders on the surface; and b) Cell sorter: A BD FACSAria™ Fusion Flow Cytometer (BD Biosciences, San Jose CA) was used to seed the naïve and transfected cell populations as single cells in 96-well plates. Cells were detached by adding Accutase™ to the cell monolayer and incubating the cells at 37 °C for 5 min. Suspended cells were pelleted at 600 rpm for 5 min and resuspended in 10 % Accumax™ and 20 % FBS in PBS to prevent cells from aggregating. Cell sorter was programmed to seed single cells in each well of a 96-well plate (in triplicates). This approach was used to quantify the percentage of the cells transfected using each transfection agent.

For both approaches, cell growth was monitored, and cell colonies were collected for DNA extraction, as described before. The 96-well plates seeded by cell sorter and the cells isolated by cylinders were screened to identify transfected populations. For this purpose, the cell population of each well (or cylinder) was separately collected, DNA was extracted, and PCR was performed. Each sample was tested by T7EI by mixing the amplicon of the sample with the amplicon of the naïve population of the cells (similar to the approach taken with mixing Controls A and B) so the missense would be detectable. Transfected cells were selected and were prepared for sequencing. PCR amplicons were submitted to Retrogen Inc. for Next Generation Sequencing (NGS).

3. Results and discussion

Toxicity. We have previously reported minimal toxicity of siRNA delivery via PLANAs in MDA-MB-231 TNBC cell line (Hall et al., 2021); however, we started by exploring the toxicity of PLANAs for two reasons: First, as a proof-of-concept study, we decided to use HEK293 cells as a standardized cell line for studies on CRISPR/Cas9 transfection efficiency; secondly, CRISPR/Cas9 reverse transfection is generally considered a more effective approach (Romero et al., 2022) and therefore, unlike the previous study that delivered siRNA using forward transfection, we needed to evaluate the potential toxicity using this approach to transfection.

Toxicity experiments were performed using four different concentrations for total RNA delivered (2.5–20 nM), which results in a corresponding increase in the concentration of each of the other nanoparticle components. Fig. 1 summarizes the cell viability in HEK293 cells after exposure to each RNA concentration delivered by Lipofectamine™ CRISPRMAX™ or PLANAs. While a slight decrease in cell viability was noticed at 10 and 20 nM total RNA delivered for Lipofectamine™ CRISPRMAX™, no significant difference was observed for this delivery system. With forward transfection, PLANAs showed minimal to no toxicity in the explored RNA concentrations, which was similar to our previous observation with siRNA delivery. However, a significant drop in cell viability was observed with reverse transfection. The percentage of viable cells was 85.5, 67.2, and 51.4 % after exposure of HEK293 cells to 5, 10, and 20 nM of total RNA delivered by PLANAs ($P < 0.05$, 0.005, and 0.0005, respectively). Our database search did not reveal any reports indicating higher toxicity for the reverse transfection approach compared to forward transfection, except a report from Promega company (Madison, WI) indicating higher toxicity for reverse transfection of plasmids with Lipofectamine™ in HEK293 cells (Hook and Schagat, 2023).

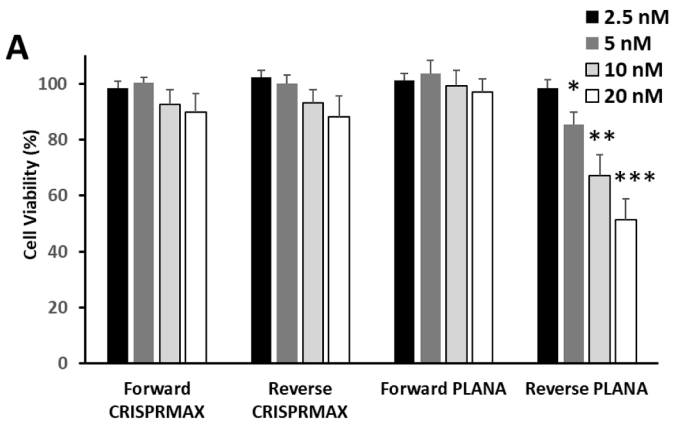

Fig. 1. Toxicity of CRISPR/Cas9 RNP delivery: RNPs were delivered by Lipofectamine™ CRISPRMAX™ to HEK293 cells via forward and reverse transfection approaches and delivering four different total RNA concentrations. PLANAs showed significant toxicity with reverse transfection. Data represents the mean ($n = 3$), and the error bars indicate standard deviation. *, **, and *** indicate P values of < 0.05, 0.005, and 0.0005, respectively, comparing the cell viability (%) of reverse transfection study groups compared to the forward transfection counterparts.

However, a correlation between efficiency and toxicity is relatively common in the field of delivery. For example, it is well-known that high molecular polyethyleneimine (PEI) is generally both more effective and more toxic than low molecular PEI (Wen et al., 2009).

Due to the significant toxicity of CRISPR/Cas9 reverse transfection via PLANAs in HEK293 cells, we investigated the addition of polyethylene glycol (PEG) to the composition of these nanoparticles. PEGylation has been reported as a strategy to reduce the toxicity of different delivery systems due to the hydrophilic nature of the polymer (Casettari et al., 2010; Luong et al., 2016; Mattheolabakis et al., 2014; Shi et al., 2021; Zhang et al., 2014; Zheng et al., 2012). In lipid-containing nanoparticles (including lipid nanoparticles or LNPs), the common strategy is to conjugate the PEG to one of the lipid components of the delivery system (Suzuki and Ishihara, 2021). We selected DOPE and cholesterol and PEGylated counterparts (with PEG 2000 and 5000 Daltons) as two major lipid components to explore the effect of PEGylation on the observed toxicity of PLANAs. The level of PEGylation was controlled by adjusting the molar ratio of PEGylated lipid and non-PEGylated lipid in each formulation.

Fig. 2 summarizes the toxicity of PEGylated and non-PEGylated PLANAs in HEK293 cells. Using Cholesterol-PEG conjugates and cholesterol with molar ratios of 1:3, 1:1, and 3:1 (represented as 25 %, 50 %, and 75 % PEGylation in the graph), showed a progressive improvement of the toxicity of the reverse transfection using PLANAs for both molecular weights of PEG. For cholesterol-PEG2000, significant toxicity was still observed at 25 % PEGylation for 10 and 20 nM total RNA delivered (the level of significance was reduced); however, at 50 % PEGylation level with 2000 Daltons PEG, only the highest concentration of total RNA caused a significant decrease in viability of HEK293 cells ($p < 0.05$). With 75 % PEGylation with PEG2000, no significant effect on cell viability was observed after reverse transfection. PEGylation with PEG5000 showed a similar trend, and the only difference was that no significant toxicity was detected at 50 % or 75 % PEGylation (Fig. 2A). Using DOPE as the PEG-carrying lipid also created similar trends. Using PEG2000, significant toxicity after reverse transfection was only detected at 25 % PEGylation and no significant decrease in viability was observed at 50 % PEGylation. PEGylation with PEG5000 created the same results for DOPE-PEG as was observed with cholesterol-PEG (Fig. 2B).

The observed results align with previous reports on the effect of PEGylation on toxicity and confirm the efficiency of this approach in

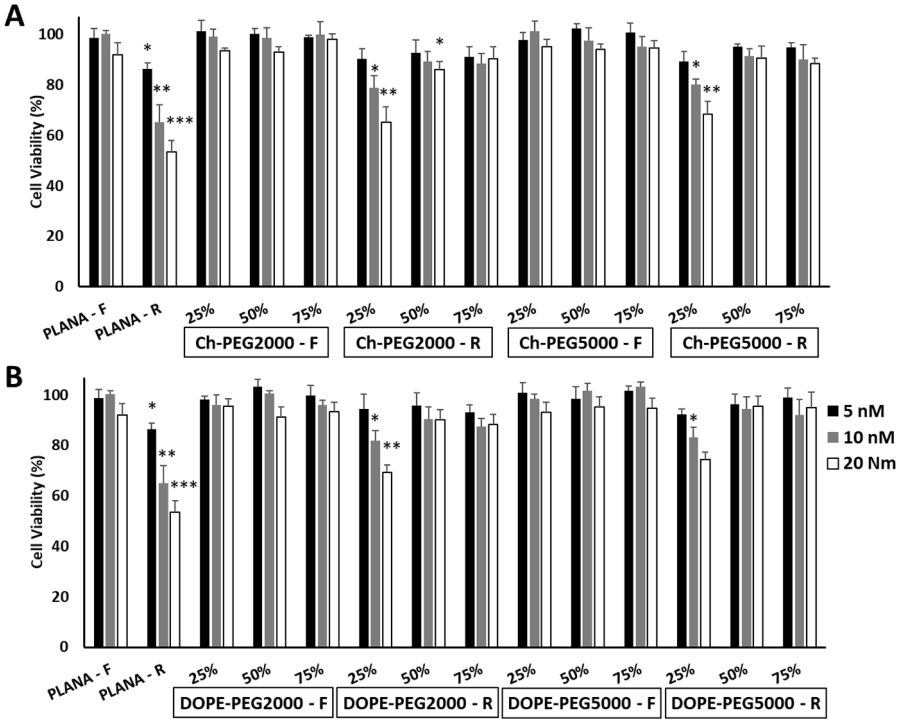

Fig. 2. Toxicity of CRISPR/Cas9 RNP delivery with PEGylated PLANAs: RNPs were delivered by non-PEGylated and PEGylated PLANAs to HEK293 cells via forward (F) and reverse (R) transfection approaches, delivering three different total RNA final concentrations (5, 10, and 20 nM). While non-PEGylated PLANAs showed significant toxicity with reverse transfection, PEGylation using two molecular weights of PEG (2 and 5 kgdaltons) decreased the observed toxicity. Data represents the mean ($n = 3$), and the error bars indicate standard deviation. *, **, and *** indicate P values of < 0.05, 0.005, and 0.0005, respectively, comparing the cell viability (%) of reverse transfection study groups compared to the forward transfection counterparts.

reducing the toxicity observed with the reverse transfection approach. The lowest PEGylation level (25 %) did not improve the safety profile sufficiently, and at least 50 % PEGylation of the "carrier" lipid seems to be required. Also, the advantage of using the higher PEG molecular weight was marginal at best and did not improve the safety profile significantly. To confirm this observation, we also investigated the toxicity of PLANAs and PLANA-PEGs in delivering siRNA to HEK293 cells using forward and reverse transfection. Please see the Supplementary information. Interestingly, reverse transfection with siRNA in HEK293 cells also showed signs of toxicity with non-PEGylated PLANAs (despite no significant toxicity with forward transfection). For PEG2000, PEGylation at 25 % level decreased the toxicity observed, while increasing the ratio of PEGylated to non-pegylated lipids (50 and 75 % levels) completely eliminated any significant decrease in cell viability. A similar trend was observed for PEG5000, except that no sign of toxicity was observed for DOPE-PEG5000, even at 25 % PEGylation level (Supplementary Fig. 2). These results again confirmed PEGylation as a viable approach to improve the safety profile of PLANAs for reverse transfection.

Encapsulation efficiency. As previously reported, selected PLANA formulations showed more than 95 % encapsulation efficiency for siRNA by quantifying the free siRNA via a SYBR Green II Dye exclusion assay (Hall et al., 2021). On the other hand, multiple reports have indicated the negative effect of PEGylation on the encapsulation of hydrophilic cargo in nanoparticles, which could be due to increased permeability of the lipid membrane of the nanoparticle (due to insertion of PEG in the particle) and leakage of the encapsulated drug (Hashizaki et al., 2005; Nicholas et al., 2000). However, this could be avoided if the PEG is placed on the surface of the particle, facing the surrounding environment (for example by grafting the PEG on the surface of pre-formed particles) (Shi et al., 2021). Therefore, we used siRNA as a model nucleic acid to investigate the effect of PEGylation on encapsulation efficiency. Using siRNA instead of CRISPR/Cas9 enabled us to use a simple dye exclusion method that detects free RNA (Cas9 complexed with RNA in the RNPs might interfere with this approach).

Fig. 3 summarizes the results of the encapsulation efficiency study. Overall, PLANAs incorporating cholesterol-PEG showed a more significant effect on encapsulation efficiency. In fact, the only PLANA incorporating cholesterol-PEG that did not show a decline in encapsulation compared to non-PEGylated PLANA was the PLANAs incorporating cholesterol-PEG2000 at 25 % level. The most significant effect was seen with cholesterol-PEG5000 at 75 % PEGylation level (with ~ 82 % encapsulation efficiency). On the other hand, none of the PLANAs containing DOPE-PEG2000 showed a significant decrease in the encapsulation efficiency at the PEGylation levels included. When DOPE was used as the PEG-conjugated lipid, significant drop in encapsulation efficiency was only observed with PEG5000 at 50 and 75 % PEGylation (~93 and 89 % encapsulation, respectively; Fig. 3). The enhanced effect on encapsulation efficiency with higher PEG molecular weight and increased mole fraction for PEG-conjugated lipid have both been previously reported (Shi et al., 2021). As mentioned before, the lower effect of DOPE-PEG on encapsulation efficiency compared to PLANAs incorporating cholesterol-PEG could be an indication of either lower incorporation of the PEG-conjugated lipid in nanoparticles or a higher localization of PEG on the outer surface of the PLANAs. We investigated this further by quantifying the surface charge of the particles.

ʒ-Potential. The surface charge of PLANAs was also quantified using siRNA as the model nucleic acid, and the results are summarized in Fig. 4. The original PLANA formulation (non-PEGylated; ~26 mV) was used as the reference point to evaluate the effect of PEGylation on the surface charge of the nanoparticles. Incorporation of cholesterol-PEG at 25 % PEGylation level did not significantly affect the ʒ-Potential of the PLANAs; however, increasing the PEGylation level to 50 and 75 % did decrease the ʒ-Potential significantly ($p < 0.05$). The most significant drop in the surface charge was observed for 75 % PEGylation (14.8 and 15.0 mV for PEG2000 and PEG5000, respectively). PLANAs

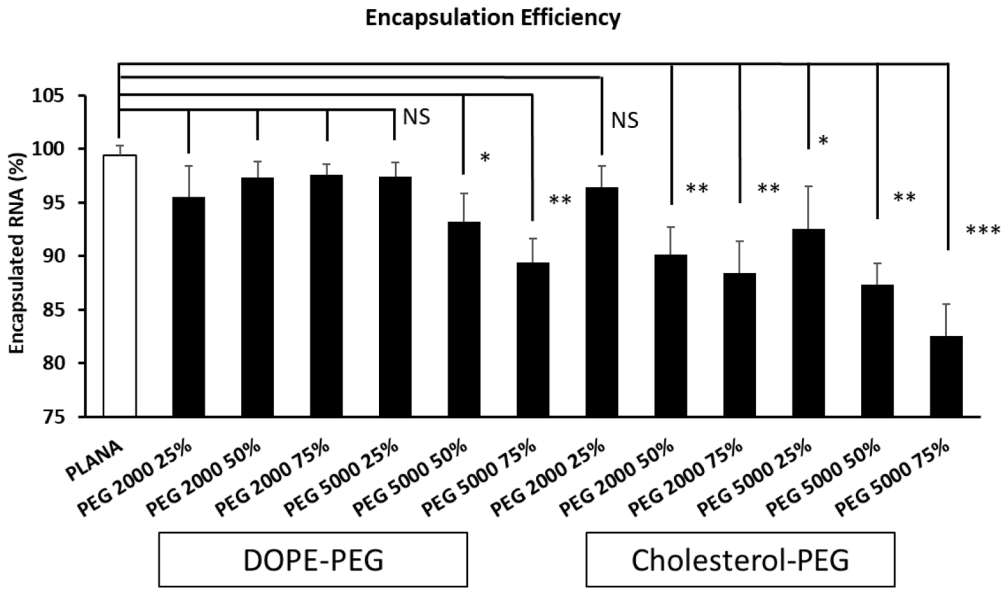

Fig. 3. Effect of PEGylation on encapsulation efficiency: siRNA was encapsulated in non-PEGylated and PEGylated PLANAs, and the free siRNA was quantified by dye exclusion assay. Conjugating PEG to cholesterol decreased encapsulation significantly for most of the study groups, while such significant effect was not seen with DOPE-PEG2000 and was less significant with DOPE-PEG5000. Data represents the mean (n = 3), and the error bars indicate standard deviation. *, **, and *** indicate P values of < 0.05, 0.005, and 0.0005, respectively, comparing the encapsulated siRNA in PEGylated to the non-PEGylated PLANAs (NS = not significant).

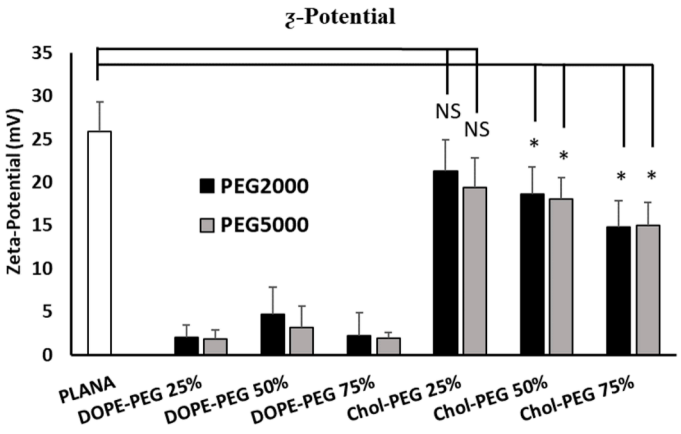

Fig. 4. Effect of PEGylation on ʒ-Potential (Zetasizer): Conjugating PEG to DOPE had a much more drastic effect on the surface charge at all PEGylation percentages. Data represent the mean (n = 3), and the error bars indicate standard deviation. * P value of < 0.05 compared to the non-PEGylated nanoparticles. The significance level for DOPE-PEG group was $P < 0.0005$ for all the study groups (NS = not significant). .

incorporating DOPE-PEG, on the other hand, showed a drastic drop in ʒ-Potential, even at the lowest percentage of PEGylation. The maximum and minimum surface charges observed within this group were 4.7 and 1.9 for DOPE-PEG2000 at 50 % PEGylation and DOPE-PEG5000 at 75 % PEGylation, respectively. While the surface charge of all DOPE-PEG groups was significantly lower than non-PEGylated PLANAs ($P < 0.0005$), there was no significant difference among the DOPE-PEG groups, regardless of the molecular weight of PEG or the percentage of PEGylation (Fig. 4).

The reducing effect of PEGylation on ʒ-Potential (positive or negative charges) has been reported. In 2020, Mahmood et al. used a Box-Behnken Design to optimize the formulation of PEGylated nanoparticles encapsulating acyclovir by adjusting the proportion of lecithin, chitosan, and PEG incorporated into the formulation (Mahmood et al., 2020). The analysis performed by Design-Expert® Software showed a negative effect of PEG proportion on the zeta potential of the nanoparticles. In 2019, Machado Cruz et al. studied the effect of PEGylation on the characteristics of negatively charged itraconazole nanoparticles, and interestingly, they reported a reduction of negative charge (from –30.1 mV to a minimum of –10.4 mV) as a result of PEGylation (Machado Cruz, Santos-Martinez, and Tajber, 2019). Our results suggest that the PEGylation via conjugation of PEG to DOPE has a more drastic effect on the surface charges. Taking the results of encapsulation efficiency evaluation studies as well, we concluded that PEGylation of PLANAs via DOPE conjugation would result in a more efficient coating of the surface of the nanoparticles with PEG and continued the study using this approach.

Cell internalization. Internalization of CRISPR/Cas9 into the target cells is the first step in transfection. ATTO-labeled tracrRNA was used to track the CRISPR/Cas9-loaded PLANAs and Lipofectamine™ CRISPRMAX™ (as positive control). Using flowcytometry, we quantified the mean fluorescent signal for the entire population of cells and the percent of the cells categorized as fluorescent-positive based on the gates defined and calibrated for cells exposed to free CRISPR/Cas9 (as a negative control). As expected, loading CRISPR/Cas9 RNPs in Lipofectamine™ CRISPRMAX™ or PLANAs (PEGylated or not) significantly increased both quantified values in HEK293 cells (Fig. 5). The difference in the average of the fluorescent signal for the CRISPRMAX and non-PEGylated PLANAs was not significant (557 vs. 531 A.U., respectively). PEGylation of PLANAs via conjugation of PEG to DOPE did not significantly affect the mean fluorescence for PLANA-PEG2000 at 25 or 50 % PEGylation level, or for PLANA-PEG5000 at 25 % PEGylation level. Increasing the PEGylation to 75 % for PEG2000, however, decreased the mean fluorescence to 408 A.U. ($P < 0.05$). Also, the decrease in mean fluorescence was significant for 50 and 75 % PEGylation with PEG5000 (415 and 375, respectively; $P < 0.05$ and < 0.005, respectively; Fig. 5A). Interestingly, the same trend was not observed for the percentage of fluorescence-positive cells. Cells exposed to the non-PEGylated PLANAs showed a higher percentage of fluorescence-positive cells compared with cells exposed to Lipofectamine™ CRISPRMAX™ ($P < 0.005$). On the other hand, while there was a slight decrease observed in the percentage of fluorescence-positive cells with an increase in PEGylation level (especially for the 75 % PEGylation), no significant difference was observed between the percentages recorded for any of the PEGylated PLANAs and the non-PEGylated nanoparticles (Fig. 5B).

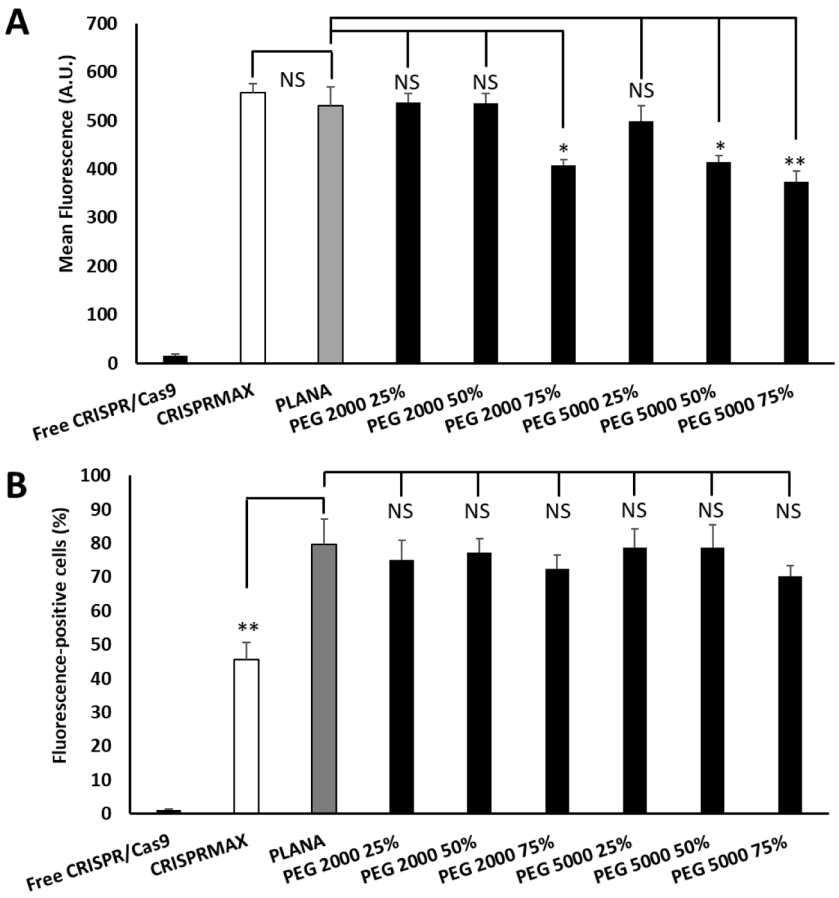

Fig. 5. Effect of PEGylation on cellular uptake of CRISPR/Cas9 RNPs using reverse transcription: A negative effect on mean fluorescence (A) and percentage of cells with fluorescence (B) was noticed in higher PEGylation levels. Data represents the mean ($n = 3$), and the error bars indicate standard deviation. * and ** indicate P values of < 0.05 and 0.005, respectively (NS = not significance).

PEGylation of nanoparticles is generally considered to limit the interaction with cell membrane and therefore, the cellular internalization of the nanoparticles, which might be attributed to the hydrophilic nature of the polymer (Romberg et al., 2008). For example, in 2013, Komeda et al. reported that cleavage of PEG lipids from liposomes would enhance cellular internalization in HeLa cells (Komeda et al., 2013). In 2004, Mishra et al. reported that PEGylation of β-cyclodextrin-containing polymers reduced cellular internalization in BHK-21 cells (Mishra et al., 2004). A similar effect has been reported for gold nanoparticles (Soenen et al., 2014). A review article published in 2017 provides numerous examples of how "cleavable" PEG would enhance cellular internalization by losing PEG before interaction with cell membrane (Fang et al., 2017).

Considering the evidence in the literature, the negative effect of PEGylation on cellular internalization is not surprising, and in fact, is another confirmation for the localization of PEG molecules on the surface of the nanoparticles. However, the advantages of PEGylation (reducing toxicity in this case) should outweigh this negative effect. While this negative effect was insignificant regarding the percentage of cells that internalized RNPs, the mean fluorescent was reduced significantly for 75 % PEGylation with PEG2000 and for 50 and 75 % PEGylation with PFG5000. Based on these results, we decided to continue the PEGylation with DOPE-PEG2000 at 50 % PEGylation level.

Confocal microscopy was performed to visualize the cellular internalization of the CRISPR/Cas9 RNPs via Lipofectamine™ CRISPRMAX™, non-PEGylated PLANAs and the PLANA-DOPE-PEG2000 at 50 % PEGylation (Fig. 6). Exposure of cells to free RNPs did not detect any signal for ATTO-labeled tracrRNA, which is not surprising due to the negligible cellular internalization of nucleic acids. However, significant internalization was observed for all delivery systems included in the study.

Transfection. To detect the transfection of HEK293 cells with CRISPR/Cas9 RNPs targeting HPRT as a model protein, we used T7 endonuclease I (T7EI) assay which has been shown to be the preferred method to detect insertions or deletions of two base-pairs (bp) that could be created as a result of Non-homologous end joining (NHEJ) by CRISPR (Vouillot et al., 2015). To validate the approach, Control A and mixture of Controls A and B were included in all transfection studies. Control A is a homoduplex (710 bp long), and therefore, cleavage by T7EI is not expected. Control B differs by a 6-base-pair deletion. Mixing Controls A and B creates homoduplexes and heteroduplexes as the result of reannealing of the PCR products. Therefore, in this mixture, in addition to the original 710 bp band, two extra bands of 442 and 268 would appear due to the digestion of heteroduplexes by the endonuclease.

Exposure to free RNPs (as negative control) did not create cleavage in the PCR amplicons treated with T7EI (Fig. 7). Clear signs of cleavage, however, were observed for CRISPR/Cas9 delivery via Lipofectamine™ CRISPRMAX™, PLANAs, and PLANA-PEG (incorporating DOPE-PEG2000 at 50 %). Extra bands at 471 and 198 bp were observed for all study groups. These results show comparable transfection efficiency for PLANAs and PEGylated PLANAs compared to the commercial transfecting agent. Supplementary Fig. 3 presents a sample image of a transfection experiment including cells exposed to normal saline, "Blank" PLANA-PEGs (formed without CRISPR/Cas9), PLANA-PEGs delivering Negative Control (scrambled) crRNA (NC), PLANA-PEGs delivering CRISPR/Cas9 targeting HPRT, Free RNPs, "Blank" Lipofectamine™ CRISPRMAX™ (reagent without CRISPR/Cas9), Lipofectamine™ CRISPRMAX™ delivering Negative Control crRNA (NC),

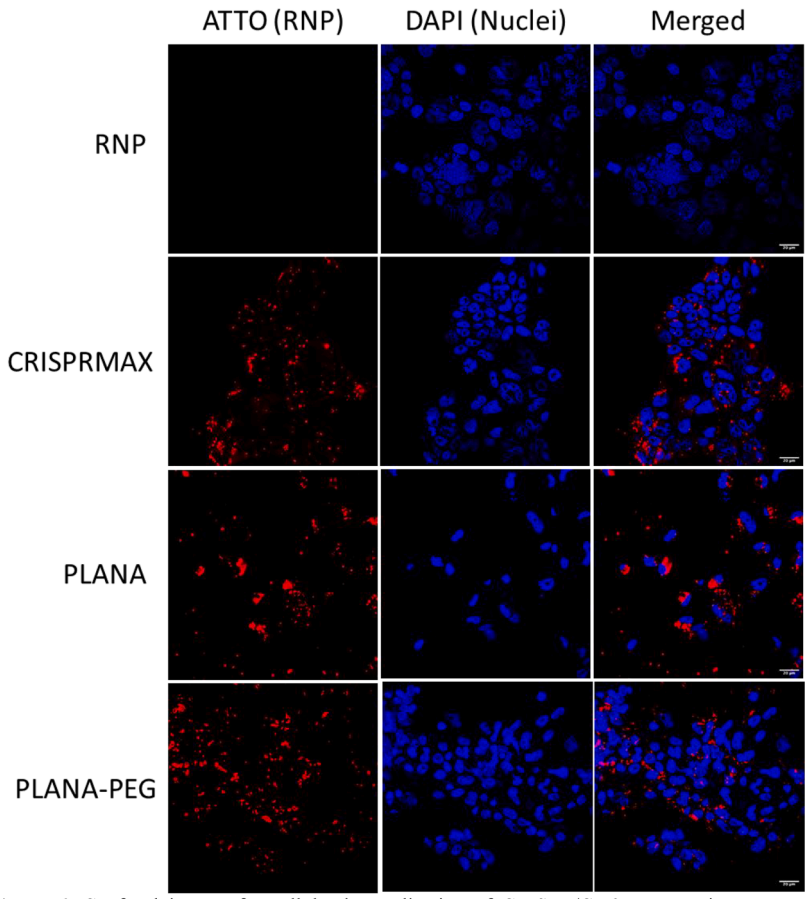

Fig. 6. Confocal images for cellular internalization of CRISPR/Cas9 RNPs using reverse transcription: Red and blue signals represent ATTO-labeled tracrRNA and DAPI (used to stain nuclei), respectively. The PLANA-PEG was prepared using DOPE-PEG2000, incorporated at 50 % level.

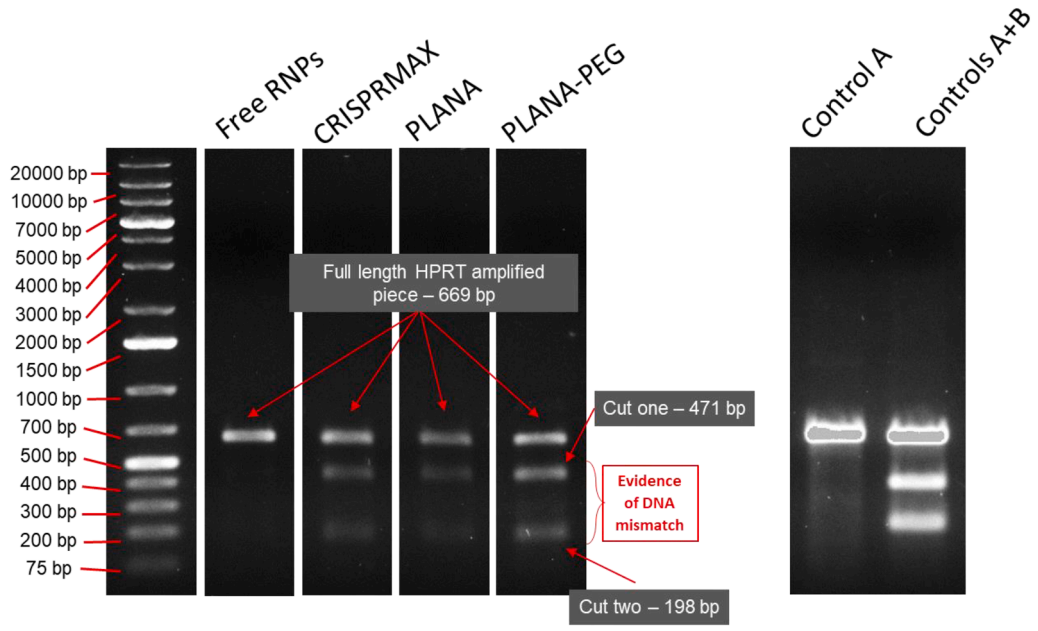

Fig. 7. Detection and cleavage of mismatched DNA using T7 endonuclease 1: A single 669 base-pair band indicates intact HPRT DNA, while appearance of two extra bands (471 and 198 base-pairs) confirms transfection. Control A and the mixture of Control A and B were used as negative and positive controls, respectively.

Lipofectamine™ CRISPRMAX™ delivering CRISPR/Cas9 targeting HPRT, Control A, and mixture of Controls A and B, respectively. Lack of cleavage is clearly observed for all the study groups except the two delivering CRISPR/Cas9 targeting HPRT.

Additionally, the percentage of the alleles with indels was calculated based on the single cells seeded in 96-well plates using the sorter. After

screening the population in each well, percentage of the cells (out of 96 well populations) transfected was calculated for RNPs delivered by Lipofectamine™ CRISPRMAX™, PLANA, and PLANA-PEG, and the results are summarized in Fig. 8. Delivering RNPs with Lipofectamine™ CRISPRMAX™ yielded ~%21 transfection rate. PLANAs yielded ~%26 transection, which was not significantly different than the rate with Lipofectamine™ CRISPRMAX™, despite the slight increase. Using PEGylated PLANAs yielded ~%35 transection, which was significantly higher than both Lipofectamine™ CRISPRMAX™ and PLANAs ($P < 0.005$ and 0.05, respectively). This was the only quantitative analysis of the transfection rate and percentage of alleles with indels that was performed, which indicates the higher efficiency of the PLANA-PEG nanoparticles in addition to their desirable safety profile compared to the original PLANA formulations.

Sequencing. In order to confirm the transfection of the cells and the creation of the indels, DNA of the cells treated with free RNPs or with RNPs delivered by Lipofectamine™ CRISPRMAX™ or PLANAs were extracted from cells cloned to create pure populations of transfected cells. The sequence of the PCR amplicons was determined by Next Generation Sequencing (NGS) performed by Retrogen Inc. (San Diego, CA). The reported sequences were matched with the expected sequence using the ApE-A plasmid Editor 2.0.49.0 software. Fig. 9 summarizes sample sequencing alignments for cloned cells exposed to free RNPs targeting HPRT (Fig. 9A), and the same RNPs delivered by Lipofectamine™ CRISPRMAX™ (Fig. 9B–D) or PLANA-PEG (incorporating DOPE-PEG2000 at 50 % PEGylation; Fig. 9E–G). All alignments included N (representing "not identified") instead of nucleic acids at the beginning and end of the PCR amplicons, which might be an indication for less-than-optimal sample clean up (to remove primers and/or any other sequence other than the PCR result) and can be ignored. The yellow highlight in the HPRT DNA sequence indicates the three nucleotides (CCT) before the targeted site by crRNA, which is the expected site for the mismatch. The crRNA-targeted site is underlined. For the cells exposed to free RNPs no mismatch is detected at the targeted site, as expected. Interestingly, the misalignments noted for the transfected cells covered a variety of the expected mutations. In cells exposed to RNPs delivered by Lipofectamine™ CRISPRMAX™, deletion of two nucleotides (T and C) at positions 199 and 200 (Fig. 9B), deletion of four nucleotides (TAGA) at positions 202–205 (Fig. 9C), and addition of three nucleotides (ATT) after position 200 (Fig. 9D) were among the observed misalignments. Similarly, for RNPs delivered by PLANAs, deletion of three nucleotides (CTA) at positions 201–203 (Fig. 9E), switch from AG to GC at positions 203 and 204 (Fig. 9F), and addition of three thymines after position 200 (Fig. 9G) were observed. The sequencing results clearly show the variety of indels created in transfected cells, regardless of the delivery system used. The full alignments can be found in Supplementary Fig. 4.

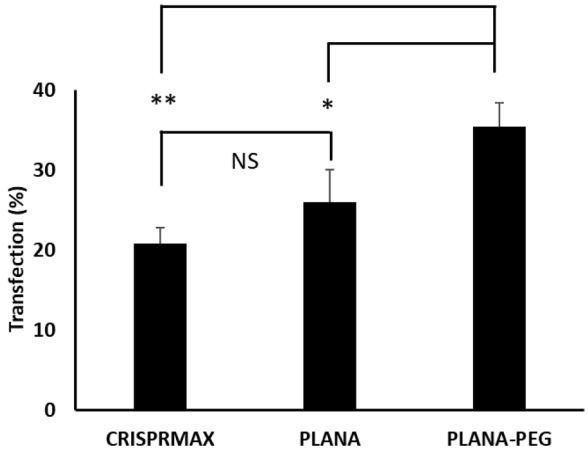

Fig. 8. Percentage of alleles with indels in HEK293 cells with RNPs targeting HPRT protein. The percentage of transfected cells was increased significantly using PEGylated PLANAs compared to both commercially available reagent and the original PLANA nanoparticles. Data represent the mean ($n = 3$), and the error bars indicate standard deviation. * and ** indicate P values of < 0.05 and 0.005, respectively (NS = not significance). .

4. Conclusion

The manuscript reports our recent attempt to use our previously reported nanoparticles, for which we coined the acronym PLANA (pronounced "PLAN A") for *in vitro* delivery of CRISPR/Cas9 ribonucleoproteins (RNPs). As a proof-of-concept study, we used a commonly used cell line for transfection studies and a model protein commonly used as a housekeeping endogenous protein. While PLANAs were efficient in internalizing the (RNPs) into the cells (demonstrated by flow cytometry and confocal microscopy), the unusual toxicity observed with reverse transfection method in the selected cell line was concerning. Therefore, PLANAs were PEGylated using two different molecular weights of PEG, three different levels of PEGylation, and using two different lipid components as "PEG-carriers". Our experiments demonstrated a decrease in toxicity with PEGylation, where the toxicity was not significant at 50 % PEGylation level with DOPE-PEG2000 even with double the concentration used for transfection studies. The encapsulation efficiency was expectedly decreased with PEGylation, which was more significant with PEG5000 and with using cholesterol-PEG (as compared to DOPE-PEG). The encapsulation efficiency remained unchanged with DOPE-PEG2000, even after replacing 75 % of DOPE molecules with the PEG-conjugated counterpart. And finally, surface charge showed a significant drop (to almost neutralized level) with DOPE-PEG (with both PEG2000 and 5000). Based on these results we concluded that PEGylation via using DOPE was a more efficient approach than using cholesterol-PEG. The internalization studies showed a slight drop in internalization which was significant with DOPE-PEG2000 at 75 % PEGylation level, and with DOPE-PEG5000 at 50 % and 75 % PEGylation. We continued the transfection studies using DOPE-PEG2000 at 50 % PEGylation level since this strategy showed little to no negative impact on the characteristics of the PLANAs. T7 endonuclease test clearly showed comparable transfection efficiency comparable to one of the leading commercial transfection agents for both PLANAs and PLANA-PEGs. However, calculation of the percentage of the transfected cells showed a significantly higher transfection rate for PEGylated PLANA formulation. Interestingly, the gene sequencing studies showed different missenses in different cloned cells with each strategy, which demonstrates a variety of possible repair errors at the guide RNA cut site. Overall, this study confirms the efficiency PLANAs in delivering CRISPR/Cas9 RNPs and the benefit of PEGylation for improved safety and efficiency of these nanoparticles.

Since PEGylation is also a strategy commonly used to increase blood circulation residence time for nanoparticles, which leads to passive targeting, we plan to use the PEGylated particles for future *in vivo* studies. The possibility of using this strategy *in vivo* could be a significant advantage over Lipofectamine™ CRISPRMAX™ and other commercial transfecting reagents. CRISPR/Cas9 delivery holds promise for transfecting cells in suspension (*e.g.*, immune cells ex vivo or even *in vivo* while in systemic blood circulation), where the reverse transfection is applicable. However, transfecting cells in a solid tissue would require forward transfection efficiency, which might further complicate *in vivo* delivery of CRISPR/Cas9. Our preliminary experiments (not reported here) showed that while the transfection efficiency of Lipofectamine™ CRISPRMAX™ dropped significantly using the forward transfection method, PLANA nanoparticles retained some of their efficiency. Further optimization of these nanoparticles in future could substantially enhance the efficiency in the forward transfection, which could be a significant achievement for *in vivo* delivery of CRISPR/Cas9 to solid tissue.

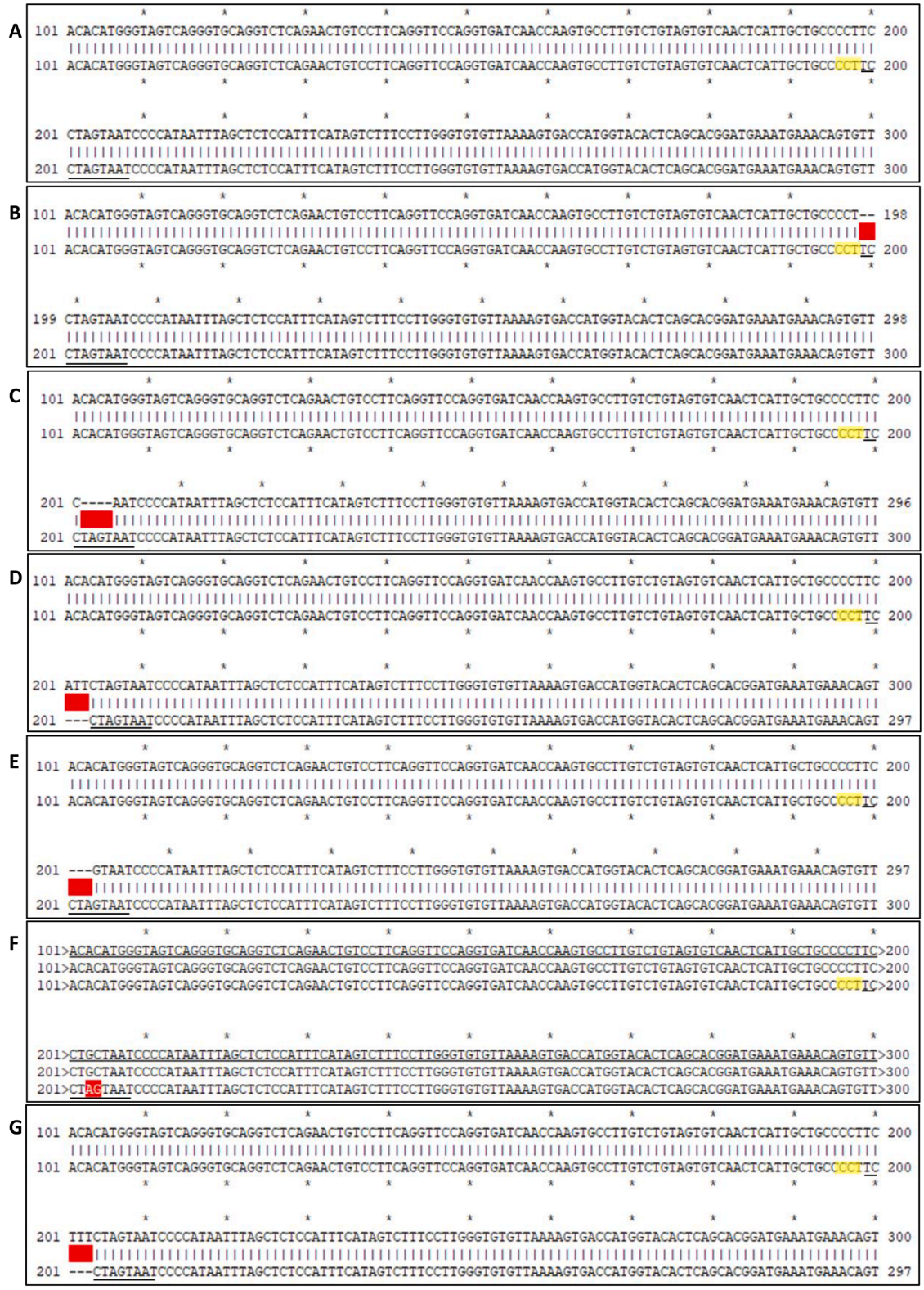

Fig. 9. Next Generation Sequencing (NGS) of cells exposed to free RNPs (A) and cloned transfected cells exposed to CRISPR/Cas9 targeting HPRT delivered by Lipofectamine™ CRISPRMAX™ (B–D) or PLANA-PEGs incorporation DOPE-PEG2000 at 50 % PEGylation (E–G): The sequence of PCR amplicon of cloned cells is at the top row and expected HPRT DNA sequence is at the bottom row for all groups. The highlighted nucleotides (CCT) indicate the site immediately before the crRNA binding site and the underlines nucleotides specify the crRNA binding site. The red highlight indicates misalignment. The full alignments can be found in Supplementary Fig. 4.

CRediT authorship contribution statement

Abdulelah Alhazza: Formal analysis, Investigation, Writing – original draft. **Parvin Mahdipoor:** Formal analysis, Investigation, Methodology, Writing – original draft. **Ryley Hall:** Formal analysis, Investigation, Methodology, Visualization. **Arthur Manda:** Formal analysis, Investigation. **Sandeep Lohan:** Formal analysis, Investigation. **Keykavous Parang:** Investigation, Methodology, Supervision, Writing – review & editing. **Hamidreza Montazeri Aliabadi:** Conceptualization, Formal analysis, Funding acquisition, Investigation, Methodology, Project administration, Resources, Supervision, Validation, Writing – review & editing.

Data availability

Data will be made available on request.

Acknowledgments

This project was supported by a Research Starter Grant in Pharmaceutics from the PhRMA Foundation. The authors would also like to thank Dr. Ajay Sharma and Dr. Jennifer Totonchy for their invaluable ideas and collaboration.

Supplementary materials

Supplementary material associated with this article can be found, in the online version, at doi:10.1016/j.ejps.2024.106708.

References

Cyranoski, D., 2016. CRISPR gene-editing tested in a person for the first time. Nature 539 (7630), 479.
Mazurov, D., Ramadan, L., Kruglova, N., 2023. Packaging and uncoating of CRISPR/Cas ribonucleoproteins for efficient gene editing with viral and non-viral extracellular nanoparticles. Viruses 15 (3).
Ma, T., Chen, X., Wang, M., 2023. Intracellular delivery of mRNA for cell-selective CRISPR/Cas9 genome editing using lipid nanoparticles. Chembiochem 24 (9), e202200801.
Liang, X., et al., 2015. Rapid and highly efficient mammalian cell engineering via Cas9 protein transfection. J. Biotechnol. 208, 44–53.
Kazemian, P., et al., 2022. Lipid-nanoparticle-based delivery of CRISPR/Cas9 genome-editing components. Mol. Pharm. 19 (6), 1669–1686.
Behr, M., et al., 2021. *In vivo* delivery of CRISPR-Cas9 therapeutics: progress and challenges. Acta Pharm. Sin. B 11 (8), 2150–2171.
Hall, R., et al., 2021. Peptide/lipid-associated nucleic acids (PLANAs) as a multicomponent siRNA delivery system. Mol. Pharm. 18 (3), 986–1002.
Do, H., et al., 2017. Difatty acyl-conjugated linear and cyclic peptides for siRNA delivery. ACS. Omega 2 (10), 6939–6957.
Casettari, L., et al., 2010. Effect of PEGylation on the toxicity and permeability enhancement of chitosan. Biomacromolecules. 11 (11), 2854–2865.
Luong, D., et al., 2016. PEGylated PAMAM dendrimers: enhancing efficacy and mitigating toxicity for effective anticancer drug and gene delivery. Acta Biomater. 43, 14–29.
Mattheolabakis, G., et al., 2014. Pegylation improves the pharmacokinetics and bioavailability of small-molecule drugs hydrolyzable by esterases: a study of phospho-Ibuprofen. J. Pharmacol. Exp. Ther. 351 (1), 61–66.
Shi, L., et al., 2021. Effects of polyethylene glycol on the surface of nanoparticles for targeted drug delivery. Nanoscale 13 (24), 10748–10764.
Zhang, F., Liu, M.R., Wan, H.T., 2014. Discussion about several potential drawbacks of PEGylated therapeutic proteins. Biol. Pharm. Bull. 37 (3), 335–339.
Zheng, J.C., et al., 2012. PEGylation is effective in reducing immunogenicity, immunotoxicity, and hepatotoxicity of alpha-momorcharin *in vivo*. Immunopharmacol. Immunotoxicol. 34 (5), 866–873.
Suzuki, Y., Ishihara, H., 2021. Difference in the lipid nanoparticle technology employed in three approved siRNA (Patisiran) and mRNA (COVID-19 vaccine) drugs. Drug Metab. Pharmacokinet. 41, 100424.
Stewart, C., Liddle, T.A., Stevenson, T.J., 2022. Abundance, efficiency, and stability of reference transcript expression in a seasonal rodent: the Siberian hamster. PLoS One 17 (10), e0275263.
Zamani, A., et al., 2020. Validation of reference genes for gene expression analysis following experimental traumatic brain injury in a pediatric mouse model. Brain Res. Bull. 156, 43–49.
Kweon, J., et al., 2018. CRISPR/Cas-based customization of pooled CRISPR libraries. PLoS. One 13 (6), e0199473.
Gasperini, M., et al., 2017. CRISPR/Cas9-mediated scanning for regulatory elements required for HPRT1 expression via thousands of large, programmed genomic deletions. Am. J. Hum. Genet. 101 (2), 192–205.
Aliabadi, H.M., et al., 2011. Impact of lipid substitution on assembly and delivery of siRNA by cationic polymers. Macromol. Biosci. 11 (5), 662–672.
Romero, J.C., et al., 2022. Oligodendrogenesis and myelination tracing in a CRISPR/Cas9-engineered brain microphysiological system. Front. Cell Neurosci. 16, 1094291.
Hook, B., Schagat, T., 2023. Reverse Transfection Using FuGENE® 6 and FuGENE® HD [cited 2023; Available from. https://www.promega.com/resources/pubhub/reverse-transfection-using-fugene-6-and-fugene-hd/#results.
Wen, Y.T., et al., 2009. A biodegradable low molecular weight polyethylenimine derivative as low toxicity and efficient gene vector. Bioconjug. Chem. 20 (2), 322–332.
Hashizaki, K., et al., 2005. Effects of poly(ethylene glycol) (PEG) concentration on the permeability of PEG-grafted liposomes. Chem. Pharm. Bull. (Tokyo) 53 (1), 27–31.
Nicholas, A.R., et al., 2000. Effect of grafted polyethylene glycol (PEG) on the size, encapsulation efficiency and permeability of vesicles. Biochim. Biophys. Acta 1463 (1), 167–178.
Mahmood, S., et al., 2020. PEGylated lipid polymeric nanoparticle-encapsulated acyclovir for in vitro controlled release and ex vivo gut sac permeation. AAPS. PharmSciTech. 21 (7), 285.
Machado Cruz, R., Santos-Martinez, M.J., Tajber, L., 2019. Impact of polyethylene glycol polymers on the physicochemical properties and mucoadhesivity of itraconazole nanoparticles. Eur. J. Pharm. Biopharm. 144, 57–67.
Romberg, B., Hennink, W.E., Storm, G., 2008. Sheddable coatings for long-circulating nanoparticles. Pharm. Res. 25 (1), 55–71.
Komeda, C., et al., 2013. A photo-triggerable drug carrier based on cleavage of PEG lipids by photosensitiser-generated reactive singlet oxygen. Org. Biomol. Chem. 11 (16), 2567–2570.
Mishra, S., Webster, P., Davis, M.E., 2004. PEGylation significantly affects cellular uptake and intracellular trafficking of non-viral gene delivery particles. Eur. J. Cell Biol. 83 (3), 97–111.
Soenen, S.J., et al., 2014. The cellular interactions of PEGylated gold nanoparticles: effect of PEGylation on cellular uptake and cytotoxicity. Particl. Particl. Syst. Character. 31 (7), 794–800.
Fang, Y., et al., 2017. Cleavable PEGylation: a strategy for overcoming the "PEG dilemma" in efficient drug delivery. Drug Deliv. 24 (sup1), 22–32.
Vouillot, L., Thelie, A., Pollet, N., 2015. Comparison of T7E1 and surveyor mismatch cleavage assays to detect mutations triggered by engineered nucleases. G3. (Bethesda) 5 (3), 407–415.